Interplay between octupole and quasiparticle excitations in ^{178}Hg and ^{180}Hg

F. G. Kondev,[1] R. V. F. Janssens,[1] M. P. Carpenter,[1] K. Abu Saleem,[1,2] I. Ahmad,[1] M. Alcorta,[1] H. Amro,[1,3] P. Bhattacharyya,[4] L. T. Brown,[1,5] J. Caggiano,[1] C. N. Davids,[1] S. M. Fischer,[6] A. Heinz,[1] B. Herskind,[7] R. A. Kaye,[1,8] T. L. Khoo,[1] T. Lauritsen,[1] C. J. Lister,[1] W. C. Ma,[3] R. Nouicer,[9] J. Ressler,[1,10] W. Reviol,[11,12] L. L. Riedinger,[11] D. G. Sarantites,[12] D. Seweryniak,[1,10] S. Siem,[1,13] A. A. Sonzogni,[1,14] J. Uusitalo,[1,15] P. G. Varmette,[3] and I. Wiedenhöver[1]

[1]*Physics Division, Argonne National Laboratory, Argonne, Illinois 60439*

[2]*Department of Physics, Illinois Institute of Technology, Chicago, Illinois 60616*

[3]*Department of Physics, Mississippi State University, Starkville, Mississippi 39762*

[4]*Department of Chemistry, Purdue University, West Lafayette, Indiana 47907*

[5]*Department of Physics, Vanderbilt University, Nashville, Tennessee 37235*

[6]*Department of Physics, DePaul University, Chicago, Illinois 60614*

[7]*The Niels Bohr Institute, 2100 Copenhagen, Denmark*

[8]*Department of Chemistry and Physics, Purdue University Calumet, Hammond, Indiana 46323*

[9]*Department of Physics, University of Illinois at Chicago, Chicago, Illinois 60607*

[10]*Department of Chemistry, University of Maryland, College Park, Maryland 20742*

[11]*Department of Physics and Astronomy, University of Tennessee, Knoxville, Tennessee 37996*

[12]*Department of Chemistry, Washington University, St. Louis, Missouri 63130*

[13]*Department of Physics, University of Oslo, N-0316 Oslo, Norway*

[14]*National Nuclear Data Center, Brookhaven, New York 11973-5000*

[15]*Department of Physics, University of Jyväskylä, P.O. Box 35, 40351 Jyväskylä, Finland*

(Received 27 April 2000; published 5 September 2000)

Excited structures in the $Z=80$, ^{178}Hg ($N=98$), and ^{180}Hg ($N=100$) isotopes have been investigated with the Gammasphere spectrometer in conjunction with the recoil-decay tagging technique. The present data extend the previously known ground-state bands to higher spin and excitation energy. Negative parity bands with a complex decay towards the low spin states arising from both the prolate-deformed and the nearly spherical coexisting minima have been observed for the first time in both nuclei. It is shown that these sequences have characteristics in common with negative-parity bands in the heavier even-even Hg isotopes as well as in the Os and Pt isotones. These structures are interpreted as being associated at low spin with an octupole vibration which is crossed at moderate frequency by a shape driving, two-quasiproton excitation.

PACS number(s): 27.60.+j, 23.20.Lv, 23.60.+e, 25.70.Gh

I. INTRODUCTION

High-spin states in neutron-deficient Hg ($Z=80$) isotopes have been the subject of numerous investigations over the years. In the mid 1970s, Hg nuclei with mass $A\leqslant 188$ were shown to exhibit shape coexistence. Sequences of states associated with a small oblate deformation characteristic of the ground state were found to coexist with well developed level sequences associated with a prolate shape [1,2]. In the 1980s and early 1990s arrays with a modest number of Compton-suppressed Ge spectrometers became available and rather detailed level schemes were obtained which provided extensive tests of the cranked shell model (see, for example [3]). Direct information on the deformation at high spin was also derived from lifetime data (see, e.g., [4]). More recently, the most neutron-deficient Hg isotopes have received much attention. The coupling of γ-ray arrays with recoil separators made it possible to discriminate efficiently the evaporation residues of interest from the copious background originating mostly from fission, and to correlate the prompt γ radiation emitted at the target with the mass of the residues and the characteristic α decays measured at the focal plane. This so-called recoil-decay tagging technique (RDT) [5] was successfully applied to measurements in ^{178}Hg [6] and ^{176}Hg [6,7]. Together with the early work by Dracoulis *et al.* on ^{180}Hg [8], these studies have validated the mean-field calculations of Refs. [9,10] by demonstrating that below neutron number $N=102$ (mid-shell) the excitation energy of a rotational band built on a prolate, normal deformed shape increases with decreasing mass to the point where there is no longer any clear evidence for its presence at low spin in ^{176}Hg [6,7]. These data also confirm the prediction [10] that for $N<100$ the coexisting oblate ground state evolves steadily as a function of decreasing neutron number towards a spherical shape.

In these Hg nuclei, excitations based on the intruder orbitals have received considerable attention because of their ability to affect the nuclear shape. In particular, it has been shown that the prolate minimum ($\beta_2\sim 0.25$) is associated with multiparticle-hole excitations across the $Z=82$ shell gap involving the $h_{9/2}$, $f_{7/2}$, and $i_{13/2}$ proton intruder orbitals [1,2]. Furthermore, there is also evidence that the occupation of specific intruder orbitals impacts the nuclear shape significantly. Specifically, Ma *et al.* [11] have shown in ^{186}Hg that the occupation of the $1/2^+[651]$ ($g_{9/2}$) and $1/2^-[770]$ ($j_{15/2}$) neutron orbitals drives the nucleus towards an enhanced prolate deformation value of $\beta_2\sim 0.35$ which is intermediate between those associated with the normally deformed ($\beta_2\sim 0.25$) [11] and the superdeformed ($\beta_2\sim 0.50$) [12] minima. Furthermore, mean-field calculations by Nazarewicz [10] with a Woods-Saxon potential pre-

dict that, for neutron number $N<98$, the prolate minimum evolves from $\beta_2 \sim 0.25$ towards larger deformations of $\beta_2 \sim 0.50-0.56$, but the excitation energy for this minimum rises to approximately 3.5 MeV.

In addition to shape coexistence phenomena, nuclei in this region also exhibit a variety of other collective and quasiparticle excitations. For example, excited negative-parity bands, consisting of cascades of stretched quadrupole transitions linked at low angular momentum to the yrast states by strong $E1$ radiation, have been reported in many even-even Os, Pt and Hg nuclei [11,13–23]. At low spin their configurations are usually associated with an octupole vibration [13,14,16–18,20], although an interpretation in terms of quasiparticle excitations has also been proposed [15,21]. At moderate rotational frequencies ($\hbar\omega \sim 0.25$ MeV), a band interaction is usually observed and the exact nature of the crossing band remains a subject of discussion.

This paper presents new data on the neutron-deficient ^{178}Hg ($N=98$) and ^{180}Hg ($N=100$) nuclei obtained with the RDT technique. It draws particular attention to the low-lying negative-parity excitations. Specifically, it compares the observed structures with excitations in the even $^{182-186}$Hg isotopes as well as in the Os and Pt isotones. Striking similarities are noted and a consistent interpretation appears to emerge based on comparisons with model calculations. A partial account of the data on the ^{178}Hg nucleus has been published earlier [24].

II. EXPERIMENTAL PROCEDURE AND DATA REDUCTION

A. Experiments

Excited states in ^{178}Hg were populated with the ^{103}Rh(^{78}Kr,$p2n$) reaction. The 350-MeV, ^{78}Kr beam with an intensity of ~ 5 pnA was delivered by the ATLAS superconducting linear accelerator at Argonne National Laboratory. A self-supporting, ~ 0.5 mg/cm^2 thick ^{103}Rh target was used. The data on ^{180}Hg are the by-product of an experiment dedicated to the study of fusion dynamics in the vicinity of the Coulomb barrier [25]. Band structures in this nucleus were populated with compound nucleus reactions using ^{90}Zr beams at a number of energies on isotopically enriched ^{90}Zr, ^{91}Zr, and ^{92}Zr targets. A summary of the reactions used, of the characteristics of the targets, and of the beam energies can be found in Table I. In order to accommodate beam intensities as high as 5 pnA, the targets were mounted on a rotating wheel. The latter controlled the pulsing of the beam so that only the targets were irradiated. In addition, the beam was wobbled ± 2.5 mm across the target with a magnetic steerer with no loss in the FMA transmission nor in the mass resolution. Prompt γ rays were detected with the Gammasphere array [26] consisting, for these experiments, of 101 large volume escape-suppressed Ge detectors arranged in sixteen rings located at angles $\theta = 31.7°, 37.4°, 50.1°, 58.3°, 69.8°, 79.2°, 80.7°, 90.0°, 99.3°, 100.8°, 110.2°, 121.7°, 129.9°, 142.6°, 148.3°$, and $162.7°$ relative to the beam direction. The recoiling products were passed through the Argonne Fragment Mass Analyzer (FMA) [27] and were dispersed according to their mass-to-charge (m/q) ratio. A 5 μg/cm^2 thick carbon foil was located ~ 8 cm behind the target to reset the charge state distribution of the recoiling nuclei. A position-sensitive parallel grid avalanche counter (PGAC), located at the focal plane, provided the m/q information as well as time of arrival and energy-loss signals of the evaporation residues. The recoiling nuclei were subsequently implanted into a 40×40 strips (40 mm$\times$40 mm,$\sim$60 μm thick), double-sided silicon strip detector (DSSD) located 40 cm behind the PGAC. This DSSD was used not only to detect the implantation of a residue and to determine its time of arrival with respect to the prompt γ-ray flash detected by Gammasphere, but also to measure its subsequent α decay(s). For this purpose, the DSSD events were time-stamped using a 47-bit, 1 MHz clock. The high pixel segmentation of the DSSD provided effective spatial and time correlations between the implants and the following α decays. During the ^{178}Hg experiment a total of 4.7×10^7 events were written to tape either when two or more Gammasphere detectors fired in coincidence with the PGAC, or when a recoil (implant event) or charged-particle (decay event) was detected in the DSSD. The total number of events in the ^{180}Hg experiment was 4.9×10^7 under similar conditions.

TABLE I. Reactions, beam energies, and target compositions for the ^{180}Hg measurements.

Reaction	Beam energy (MeV)	Target	Abundance (%)	Target thickness (μg/cm^2)
^{90}Zr+^{90}Zr	369	^{90}Zr	97.65	550
			0.96 (^{91}Zr)	
			0.71 (^{92}Zr)	
			0.55 (^{94}Zr)	
			0.13 (^{96}Zr)	
^{90}Zr+^{91}Zr	380	^{91}Zr	89.20	560
			5.99 (^{90}Zr)	
			3.29 (^{92}Zr)	
			1.30 (^{94}Zr)	
			0.22 (^{96}Zr)	
^{90}Zr+^{92}Zr	380	^{92}Zr	95.13	550
			2.54 (^{90}Zr)	
			1.04 (^{91}Zr)	
			1.11 (^{94}Zr)	
			0.18 (^{96}Zr)	

B. Data reduction

To isolate the ^{178}Hg and ^{180}Hg residues and the corresponding prompt γ rays from the dominating background contributions originating from scattered beam, from fission products and from deexcitations in neighboring isotopes, coincidence gates were placed in the off-line analysis on (i) the time of flight of the evaporation residues from the target to the focal plane, (ii) the PGAC positions corresponding to three charge states ($q=31$, 32, and 33) of ions with the appropriate $A=178$ and 180 mass focus, and (iii) the two-

TABLE II. Alpha decay properties of the ^{178}Hg and ^{180}Hg ground states.

Nucleus	J_i^π	J_f^π	Present			Previous [29]			
			E_α (keV)	I_α (%)	$t_{1/2,\alpha}$ (s)	E_α (keV)	I_α (%)	$t_{1/2,\alpha}$ (s)	b_α (%)
^{178}Hg	0^+	0^+	6429(4)	~100	0.262(4)	6430(6)	98(2)	0.266(25)	97^{+3}_{-25}
^{180}Hg	0^+	0^+	6119(4)	~100	2.59(2)	6120(5)	99.87(3)	2.56(2)	48(9)

dimensional histogram of the energy of recoils measured in the DSSD vs the time of flight from the PGAC to the DSSD.

1. Recoil-$\gamma-\gamma$ and recoil-$\alpha-\gamma-\gamma$ events

The γ-ray data were sorted into E_γ-E_γ matrices of coincidence events occurring within a 60 ns time window. Since γ-ray emission occurs when the recoiling nuclei are in flight ($v/c \sim 4\%$), the transition energies were corrected for the Doppler shift. Background subtracted spectra were then produced for each particular cascade and were examined with the RADWARE [28] interactive software package in order to construct the level scheme. To enhance the ^{178}Hg and ^{180}Hg γ rays from those produced by other $A=178$ and 180 residues, additional $\gamma-\gamma$ coincidence matrices gated by the characteristic α lines of $E_\alpha=6430$ keV (^{178}Hg) and 6120 keV (^{180}Hg) [29] were also created. Most of the γ rays assigned to the nuclei of interest were identified in the analysis of these matrices, hereby confirming the isotopic assignment.

2. Recoil-α-time events

Two-dimensional histograms with the energies of the first generation α decays on one axis and the difference between the implantation and α-decay times on the other were constructed after matching the individual energy signals of all DSSD strips. Energy spectra gated on different regions of the time axis were then constructed and used to deduce the α-decay energies and intensities. The selection of specific time intervals significantly reduced the complexity of the α-energy spectra as well as the background due to random correlation events. Time spectra were generated for each α line and used to determine the half-life of the emitting state, using a least-squares fitting method [30].

3. Gamma-ray angular distributions and anisotropies

Angular distributions were obtained by projecting mass-gated spectra corresponding to γ rays detected in a specific ring of detectors in Gammasphere. From these spectra the intensities of the strongest lines were measured and then fitted with the usual expression

$$W(\theta)=1+A_2P_2(\cos\theta)+A_4P_4(\cos\theta), \qquad (1)$$

where A_2 and A_4 are the angular distribution coefficients (the normalization factor A_0 has been omitted for simplicity) and $P_l(\cos\theta)$ are the Legendre polynomial functions. For several weak lines only the A_2 coefficients were extracted by setting $A_4=0$. The angular distribution information was extended further by extracting the anisotropy ratio R, defined as the intensity ratio of transitions observed in the 31.7° (and the equivalent 148.3°), 37.4° (142.6°), and 162.7° detector rings to those detected in the 79.2° (100.8°), 80.7° (99.3°), and 90.0° rings. In general, values greater than unity indicate a stretched quadrupole or mixed $M1/E2$, $\Delta J=1$ transition with a positive sign for the mixing ratio, δ. Values of $R<1$ are associated with a pure dipole or mixed $M1/E2$, $\Delta J=1$ transition with $\delta<0$. These assignments were consistently checked with a number of transitions of known multipolarity in the neighboring odd-mass nuclei which received a significant population in the present measurements.

III. EXPERIMENTAL RESULTS

A. Previous studies

The α decays from the ^{178}Hg and ^{180}Hg ground states have been studied previously by several authors: see Ref. [29] for the most recent compilation and evaluation of all published work. As indicated above, Carpenter *et al.* [6] reported on the first observation of excited states in ^{178}Hg using the ^{103}Rh(^{78}Kr, $p2n$) reaction in conjunction with the RDT technique. The ground-state band was established up to 8^+ (tentatively up to 12^+). More recently, an expanded level structure of ^{178}Hg was presented by Kondev *et al.* [24]. Dracoulis *et al.* [8] identified the yrast band of ^{180}Hg up to 14^+ (16^+) and reported several other γ rays which were, however, not placed in the level scheme.

B. Alpha-decay measurements

As summarized in Table II, the present data confirm the properties of the previously reported main, $0^+\rightarrow 0^+$, α lines of ^{178}Hg and ^{180}Hg. Using the time spectra produced by gating on the 6429 and 6119 keV α lines, half-lives of $T_{1/2,\alpha}=0.262(4)$ and 2.59(2) s were obtained for the decay of the ^{178}Hg and ^{180}Hg ground states. The measured $T_{1/2,\alpha}$ values are in good agreement with those reported previously [29].

C. Level scheme construction

The level schemes of ^{178}Hg and ^{180}Hg deduced from the present study are given in Figs. 1 and 2, respectively. The assignment of γ rays to the nuclei of interest is based on the observed correlations with the characteristic ^{178}Hg and ^{180}Hg α lines, and on measured coincidence relationships with previously known transitions in these nuclei [6,8], as well as with the characteristic Hg x rays. The γ rays assigned to ^{178}Hg and ^{180}Hg are listed in Tables III and IV together with their intensities, angular distribution, and anisotropy coefficients, and adopted multipolarity. Some relative γ-ray intensities were obtained from the total projection of the recoil-

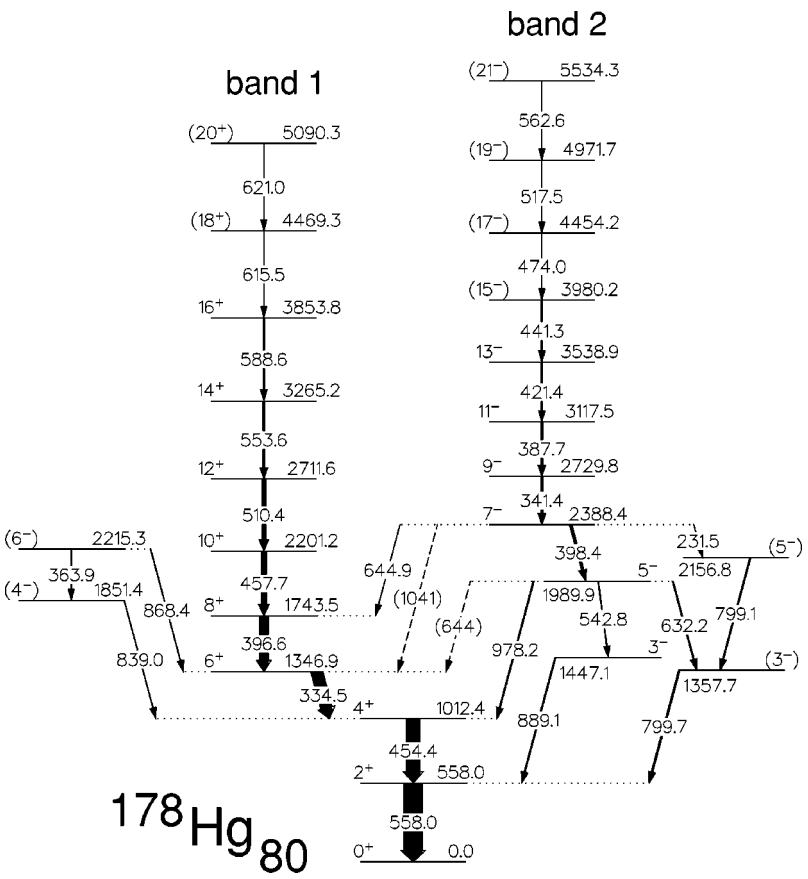

FIG. 1. Level scheme of ^{178}Hg deduced from this work. Tentative placements are indicated by dashed lines. Tentative spin-parity assignments are given in parenthesis.

$\gamma-\gamma$ matrices, others were extracted from coincidence spectra after proper normalization. Although angular correlations could affect the measured intensities (at a $\sim$10% level), no corrections were applied.

The spin and parity assignments are based mainly on the angular distribution and anisotropy information. The present measurements were not sensitive to the identification of isomeric states because the residues fly out of the focus of Gammasphere into the FMA. Hence, the character of each transition was restricted to either $E1$, $E2$, $M1$ or to the appropriate mixing of these multipolarities. Several of the assignments are tentative. These are indicated under parenthesis in Figs. 1 and 2, and in Tables III and IV. Furthermore, additional arguments such as the relative population of levels within a given band, the presence or absence of certain transitions and the band structure itself have been used to remove possible ambiguities in specific instances.

1. ^{178}Hg

As mentioned above, the ^{178}Hg level scheme has been presented in an earlier, short publication [24]. Some additional information is given below for completeness. In particular, the detailed data on intensities and multipolarities of the transitions placed in the scheme of Fig. 1 can be found in Table III. A coincidence spectrum showing the main transitions assigned to band 1 is presented in Fig. 3(a). The data confirm the observations of Ref. [6] and extend the band by four levels up to the $J^{\pi}=(20^{+})$ state. The placement and ordering of the in-band transitions are based on the observed coincidence relationships and on the measured relative intensities. The stretched $E2$ character was derived for all γ rays below the 16^{+} level from the measured angular distributions and anisotropy ratios (see Table III), thereby confirming the spin values given in Fig. 1. The multipolarity of the transitions depopulating the two highest levels in the band could not be established directly because of the weak intensities involved. Nevertheless, the assignments can be viewed as probable because of the collective character of the sequence.

Band 2 [Figs. 1 and 3(b)] has been identified for the first time in the present data and was the main subject of discussion in Ref. [24]. The $E2$ character of the first three in-band transitions is firmly established from the measured angular distributions and anisotropies. The $E2$ assignment to the higher members in the band is again based on the collective character. Remarkably, the decay out of this sequence towards the lower states is fragmented over a fair number of pathways, most of which feed levels that have not been reported previously. The odd spin, negative parity assignment to band 2 comes from the measured multipolarity of the main decay-out transitions (398.4, 644.9, 542.8, 889.1, 978.2 keV). In particular, only $J=7\ \hbar$ is possible for the 2388.4 keV level as any other spin value implies the presence of at least one higher-order ($E3$ or $M3$) γ ray. A positive parity is viewed as highly unlikely as a 1041 keV M1 transition would be expected to be four times stronger than the competing 644.9 keV γ ray (energy factor). In contrast, as discussed in detail below, the $J^{\pi}=7^{-}$ assignment agrees with the systematics based on a comparison with negative parity

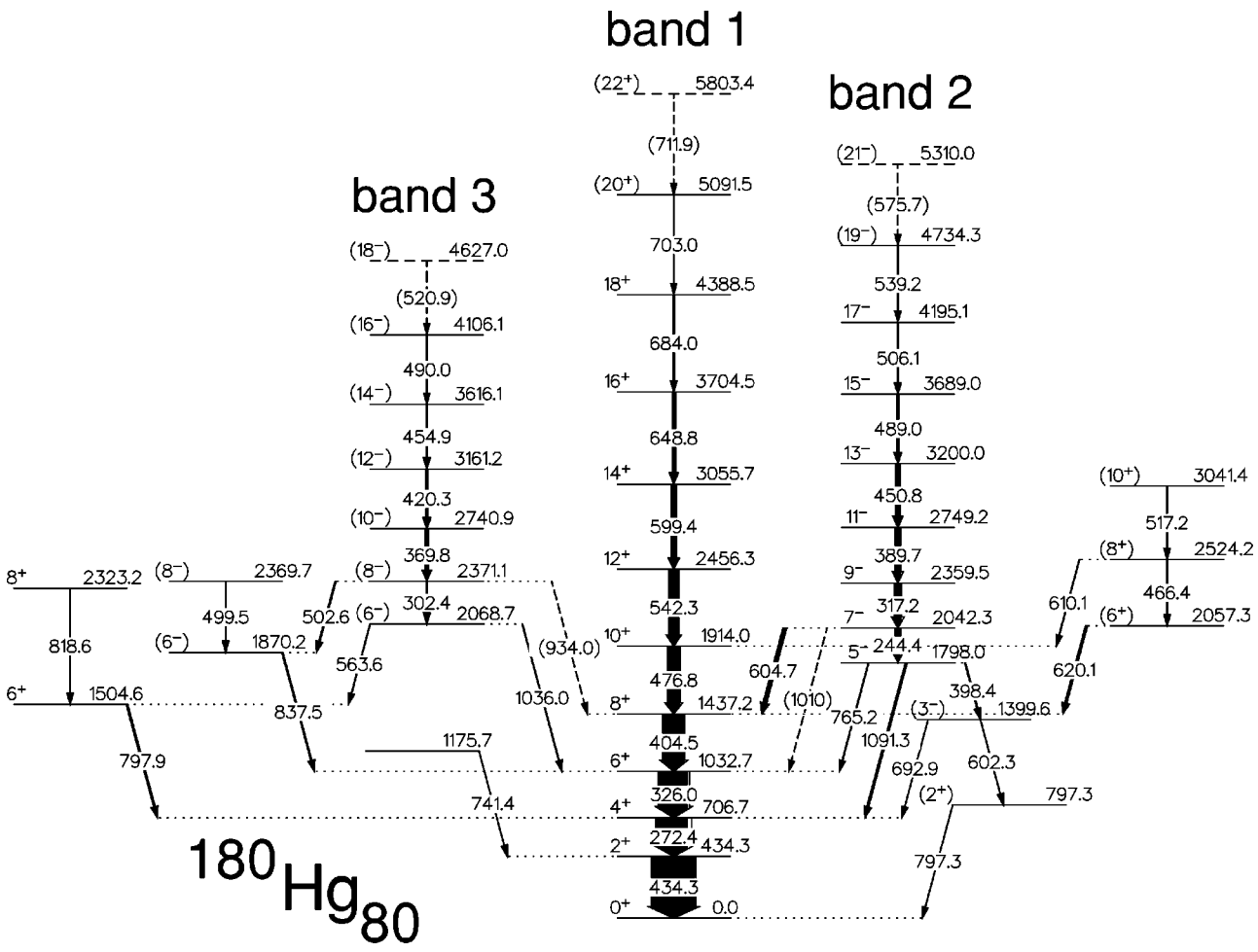

FIG. 2. Level scheme of ^{180}Hg deduced from this work. Tentative placements are indicated by dashed lines. Tentative spin-parity assignments are given in parenthesis.

bands in the neighboring nuclei. In the decay out of band 2, the J^{π} quantum numbers of the levels at 1447.1 and 1989.9 keV are firmly established while those of the states at 1357.7 and 2156.8 keV are only tentative. Finally, two other states with tentative spin and parity assignments have also been placed in the level scheme (1851.4, 2215.3 keV).

2. ^{180}Hg

A sample spectrum showing the γ rays in coincidence with the 476.8, 542.3, 599.4, 648.8, and 684.0 keV transitions located above the 8^+ level of the ^{180}Hg ground-state band is presented in Fig. 4(a). Compared to previous work [8], this band has now been extended up to the 20^+ level (tentatively 22^+). The angular distribution and anisotropy information is consistent with a stretched quadrupole character for all in-band γ rays up to the 18^+ state.

A coincidence spectrum showing γ rays associated with band 2 is presented in Fig. 4(b). This sequence is assigned odd spins and negative parity on the basis of several arguments. The angular distribution and anisotropy coefficients for the 765.2 and 1091.3 keV γ rays (Table IV) are of dipole character. This observation limits the spin value for the 1798.0 keV state to 5 $\hbar$. In addition, the $E2$ character of the 244.4 keV in-band transition and the dipole nature of the 604.7 keV line make the 7 $\hbar$ spin assignment to the 2042.3 level straightforward. The argument for the negative parity is similar to the one presented above for band 2 in ^{178}Hg, i.e., a 1010 keV $M1$ transition would be expected to be roughly four times stronger than the competing 604.7 keV γ ray (energy factor), while the experimental observation is opposite. Finally, as discussed in detail in Refs. [18,24] and as elaborated upon below, the observed decay pattern finds a natural explanation if a negative parity is assigned.

Band 3 is observed for the first time in this work. A coincidence spectum showing the main γ rays of this sequence is presented in Fig. 4(c). The proposed spin assignments are based on the measured anisotropy of a single transition (1036.0 keV) (see Table IV) and on population intensity arguments. As a result, these assignments are considered tentative. For example, the ratio of 0.68(6) between the intensities of the 369.8 keV γ ray (band 3) and the 389.7 keV transition (band 2) suggests that the spin of the 2740.9 keV level (band 3) is at least one unit less than the value of 11 $\hbar$ assigned to the 2749.2 keV level (band 2). The nonobservation of transitions from the first three in-band levels to the 4^+, 6^+, and 8^+ members of the ground-state band (e.g.,

TABLE III. Excitation energies, spins, parities, and transition energies, intensities, angular distribution coefficients, anisotropies and adopted multipolarities for band structures assigned to ^{178}Hg.

E_x (keV)	J_i^π ($\hbar$)	E_γ (keV) [a]	I$_\gamma$ (rel.) [b]	A_2/A_0	A_4/A_0	R [c]	Assignment
Band 1							
558.0	2^+	558.0	1000(17)	0.30(7)	−0.15(8)	1.36(16)	$E2$
1012.4	4^+	454.4	745(16)	0.29(7)	−0.07(12)	1.40(18)	$E2$
1346.9	6^+	334.5	611(13)	0.28(11)	−0.24(15)	1.58(22)	$E2$
1743.5	8^+	396.6	485(24)	0.33(11)	0.09(15)	1.21(12)	$E2$
2201.2	10^+	457.7	293(13)	0.27(5)	−0.12(7)	1.43(18)	$E2$
2711.6	12^+	510.4	218(9)	0.41(21)	−0.16(27)	1.52(23)	$E2$
3265.2	14^+	553.6	127(8)			1.47(25)	$E2$
3853.8	16^+	588.6	68(7)			1.51(21)	$E2$
4469.3	(18^+)	615.5	30(5)				$(E2)$
5090.3	(20^+)	621.0	<20				$(E2)$
Band 2							
2388.4	7^-	398.4	138(21)			1.47(20)	$E2$
		644.9	24(5)			0.47(18)	$E1$
		231.5	21(6)				$(E2)$
		(1041)	<10				$(E1)$
2729.8	9^-	341.4	125(7)	0.34(11)	0.00(15)	1.32(18)	$E2$
3117.5	11^-	387.8	106(7)	0.37(11)	−0.06(15)	1.45(20)	$E2$
3538.9	13^-	421.4	60(6)			1.21(18)	$E2$
3980.2	(15^-)	441.3	54(6)				$(E2)$
4454.2	(17^-)	474.0	19(9)				$(E2)$
4971.7	(19^-)	517.5	14(8)				$(E2)$
5534.3	(21^-)	562.6	<10				$(E2)$
Other levels							
1447.1	3^-	889.1	68(8)			0.83(22)	$E1$
1989.9	5^-	978.2	67(9)			0.69(20)	$E1$
		542.8	21(6)			1.24(23)	$E2$
		632.2	40(7)			1.35(23)	$E2$
		(644)	<10				$(E1)$
1357.7	(3^-)	799.7	87(8)			0.60(19)	$(E1)$
2156.8	(5^-)	799.1	47(11)				$(E2)$
1851.4	(4^-)	839.0	34(5)			1.59(26)	$(E1)$
2215.3	(6^-)	363.9	20(5)				$(E2)$
		868.4	<10				$(E1)$

[a]Energies are accurate to within 0.1–0.2 keV for the strong transitions. For weaker transitions the uncertainty may rise up to as much as 0.8 keV.

[b]Relative intensities deduced from the total projection of the recoil$-\gamma-\gamma$ matrix, as well as from coincidence projections after appropriate normalization. (See the text for details.)

[c]Angular anisotropy coefficients. (See the text for details.)

$6\rightarrow4^+$, $8\rightarrow6^+$ and $10\rightarrow8^+$) favors a negative parity assignment for band 3. It is also worth noting that the proposed assignments are consistent with the systematic features exhibited by the neighboring even-even Os and Pt isotopes [14,18,20], as well as with considerations based on the extracted alignments (see discussions below).

Additional levels at 1504.6, 1870.2, 2057.3, 2323.2, 2369.7, 2524.2, and 3041.4 keV have also been established. Unfortunately, for most of these, firm spin and parity assignments could not be obtained.

IV. DISCUSSION

Negative parity bands have been observed in a number of even-even Os, Pt, and Hg isotopes. There is, however, no consensus regarding their interpretation. Dracoulis *et al.* [14] proposed that, at low spins, these structures in ^{176,178,180}Os are built on a single-phonon octupole vibration. At higher angular momentum, these octupole bands are then crossed by two-quasiparticle excitations. A similar interpretation has also been adopted by Cederwall *et al.* [17], Kondev *et al.* [18] and de Voigt *et al.* [20] in their studies of neighboring ^{176}Pt, ^{178}Pt, and ^{180}Pt isotopes. In contrast, Popescu *et al.* [21] and Lieder *et al.* [15] proposed a pure two-quasiparticle assignment for the negative parity structures in ^{182}Pt and ^{180}Os, respectively.

In the even-even Hg isotopes, the interpretation of the observed negative parity structures may be more subtle than in the Pt or Os isotones since their susceptibility to shape

TABLE IV. Excitation energies, spins, parities, and gamma-ray energies, intensities, angular distribution coefficients, anisotropies and adopted multipolarities for level structures assigned to ^{180}Hg.

E_x (keV)	J_i^π ($\hbar$)	E_γ (keV) [a]	I_γ (rel.) [b]	A_2/A_0	A_4/A_0	R [c]	Assignment
Band 1							
434.3	2^+	434.3	1000(30)	0.28(6)	−0.06(8)	1.22(5)	$E2$
706.7	4^+	272.4	725(24)	0.24(6)	−0.12(8)	1.30(6)	$E2$
1032.7	6^+	326.0	675(22)	0.29(6)	−0.09(6)	1.28(6)	$E2$
1437.2	8^+	404.5	503(17)	0.33(7)	−0.03(10)	1.34(8)	$E2$
1914.0	10^+	476.8	282(12)	0.46(12)	−0.03(16)	1.33(15)	$E2$
2456.3	12^+	542.3	215(10)	0.37(17)	0.03(22)	1.72(23)	$E2$
3055.7	14^+	599.4	135(8)	0.43(19)		1.10(25)	$E2$
3704.5	16^+	648.8	81(5)			1.28(21)	$E2$
4388.5	18^+	684.0	31(4)			1.21(25)	$E2$
5091.5	(20^+)	703.0	10(2)				$(E2)$
5803.4	(22^+)	(711.9)	<8				$(E2)$
Band 2							
1798.0	5^-	398.4	25(5)			1.11(52)	$E2$
		765.2	17(4)			0.65(19)	$E1$
		1091.3	46(5)			0.73(14)	$E1$
2042.3	7^-	244.4	107(5)	0.31(13)		1.39(25)	$E2$
		604.7	87(7)	−0.57(29)		0.54(17)	$E1$
		(1010)	<30				$(E1)$
2359.5	9^-	317.2	154(7)	0.36(9)			$E2$
2749.2	11^-	389.7	120(6)	0.30(11)		1.26(13)	$E2$
3200.0	13^-	450.8	101(5)	0.53(20)		1.33(22)	$E2$
3689.0	15^-	489.0	50(7)			1.63(50)	$E2$
4195.1	17^-	506.1	32(6)			1.48(50)	$E2$
4734.3	(19^-)	539.2	18(5)				$(E2)$
5310.0	(21^-)	(575.7)	<10				$(E2)$
Band 3							
2068.7	6^-	563.6	15(4)				$(E1)$
		1036.0	18(4)			1.86(31)	$(E1)$
2371.1	8^-	302.4	24(4)			1.31(36)	$E2$
		502.6	29(5)				$(E2)$
		(934.0)	<10				$(E1)$
2740.9	10^-	369.8	81(6)	0.54(20)		1.24(26)	$E2$
3161.2	12^-	420.3	56(5)			1.16(26)	$E2$
3616.1	14^-	454.9	34(4)			1.34(30)	$E2$
4106.1	(16^-)	490.0	13(3)				$(E2)$
4627.0	(18^-)	(520.9)	<10				$(E2)$
Other levels							
1399.6	(3^-)	602.3	<20				$(E1)$
		692.9	<20				$(E1)$
797.3	(2^+)	797.3	<20				$(E2)$
1504.6	6^+	797.9	39(5)			1.11(13)	$E2$
2323.2	8^+	818.6	21(6)			1.37(22)	$E2$
1870.2	(6^-)	837.5	28(4)			1.13(19)	$(E1)$
2369.7	(8^-)	499.5	13(4)				$(E2)$
1175.7		741.4	<10				
2057.3	(6^+)	620.1	50(5)	0.50(11)		1.29(16)	$E2$
2524.2	(8^+)	466.4	20(7)				$(E2)$
		610.2	15(3)				$(E2)$
3041.4	(10^+)	517.2	19(3)				$(E2)$

[a]Energies are accurate to within 0.1–0.2 keV for the strong transitions. For weaker transitions the uncertainty may rise up to as much as 0.8 keV.

[b]Relative intensities deduced from the total projection of the recoil $-\gamma-\gamma$ matrix, as well as from coincidence projections after appropriate normalization. (See the text for details.)

[c]Angular anisotropy coefficients. (See the text for details.)

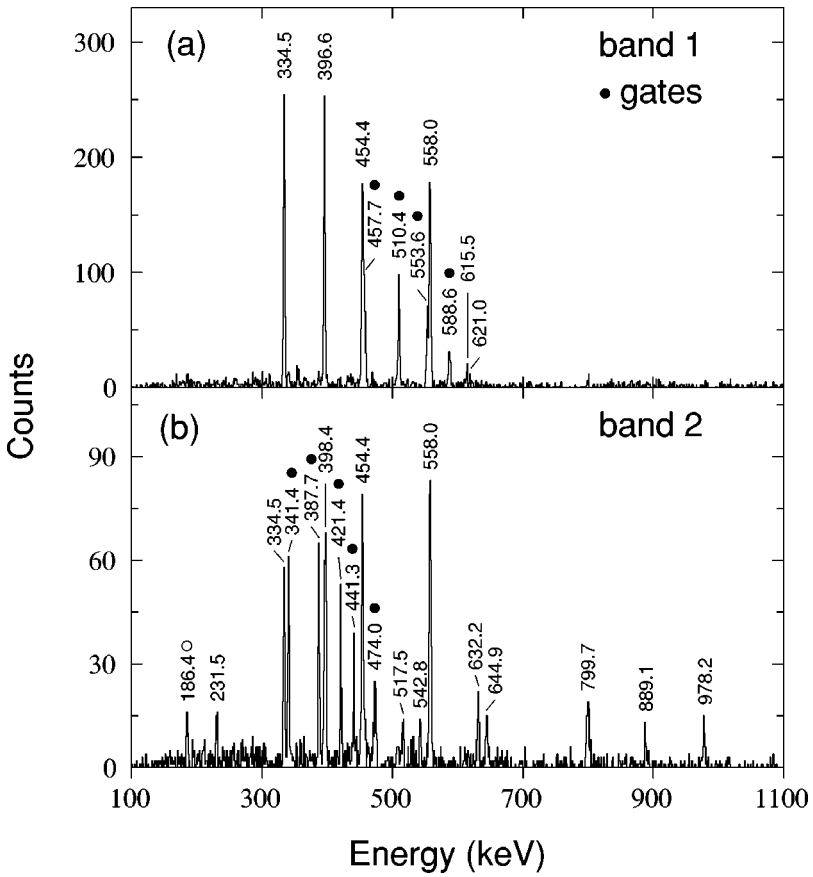

FIG. 3. Summed, background-subtracted γ-ray coincidence spectra from the recoil-$\gamma-\gamma$ matrix produced by gating on transitions in band 1 (a) and band 2 (b) in ^{178}Hg. The γ ray labeled with the open symbol is most likely a contaminant.

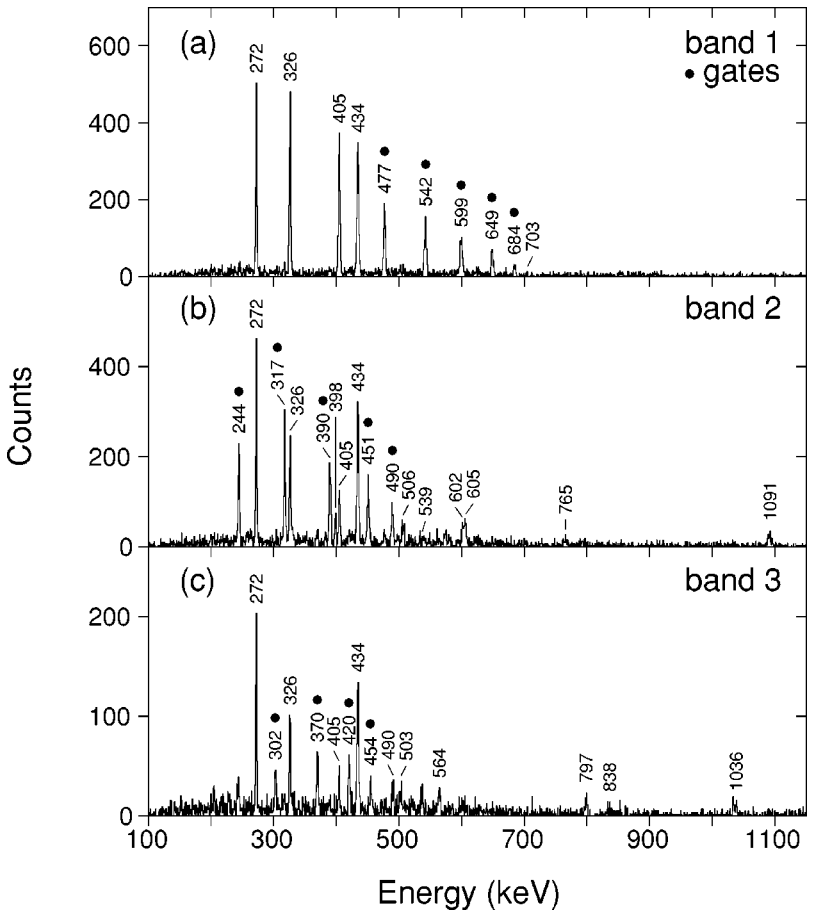

FIG. 4. Summed, background-subtracted γ-ray coincidence spectra from the recoil-$\gamma-\gamma$ matrix produced by gating on transitions in band 1 (a), band 2 (b) and band 3 (c) in ^{180}Hg.

changes needs to be taken into account. As already discussed above, Ma *et al.* [11] have shown in ^{186}Hg that the occupation of specific neutron orbitals drives the nucleus towards a so-called intermediate prolate deformation. The measured quadrupole moment $Q_0 = 10.7(1.7)$ eb [11] highlights the shape-driving effects of the intruder neutron orbitals associated with the band structure of interest. As shown in Ref. [11], the two possible configurations ($\nu^2([651]1/2 \otimes [514]7/2)$ or $\nu^2([651]1/2 \otimes [771]1/2)$) are difficult to distinguish and a firm assignment was not proposed. It is worth pointing out that while negative parity bands have also been observed in ^{182}Hg [22] and ^{184}Hg [23], they show little similarity with the intermediate deformation structure of ^{186}Hg.

The negative parity bands in both ^{178}Hg and ^{180}Hg are characterized by a number of rather distinctive features. These are

(1) The measured alignment at low frequency is ~ 3 $\hbar$;

(2) the bands undergo a subsequent alignment gain of roughly 5 $\hbar$ at the noticeably low frequency of ~ 0.21 MeV;

(3) at low spin, the $\mathfrak{I}^{(2)}$ moments of inertia are larger than the corresponding values in the respective yrast band; and

(4) the bands stand out by the complexity of their deexcitation patterns as the 7^- states decay into a large number of levels (three, possibly four). This last observation may suggest that the associated intrinsic structure is quite different from that of the yrast bands and that the decay proceeds towards most, if not all, available lower-energy levels without much selection on the basis of shape or degree of collectivity.

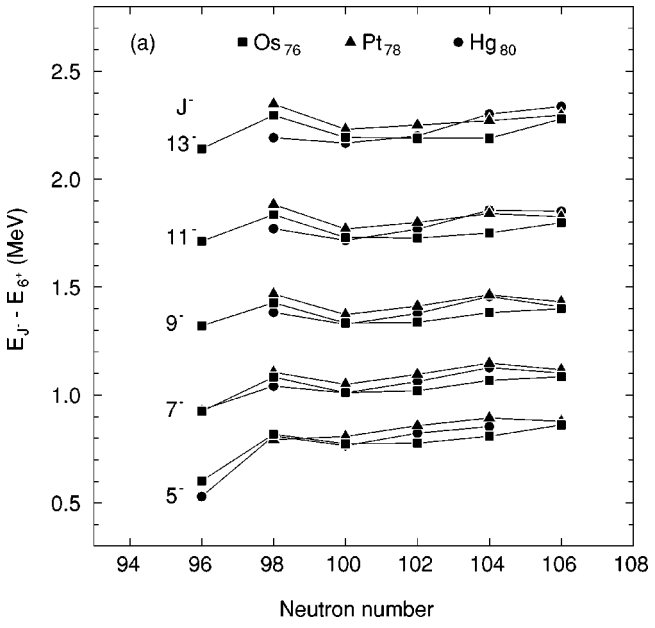

FIG. 5. Excitation energies for the 5^-, 7^-, 9^-, 11^-, and 13^- levels relative to the 6^+ member of the ground state band for the structures in Os, Pt, and Hg even-even nuclei. The data are taken as follows: ^{172}Os (side band I) [31]; ^{174}Os (side band II) [32]; ^{176}Os (band I), ^{178}Os (band I), and ^{180}Os (band I) [14]; ^{182}Os [16]; ^{176}Pt [17]; ^{178}Pt (band 2) [18]; ^{180}Pt (band I) [20]; ^{182}Pt (band 5) [21]; ^{184}Pt (band 5) [37]; ^{176}Hg [7]; ^{178}Hg (band 2) (present work); ^{180}Hg (band 2) (present work); ^{182}Hg (band 3) [22]; ^{184}Hg (band 6) [23]; ^{186}Hg (band 8) [11].

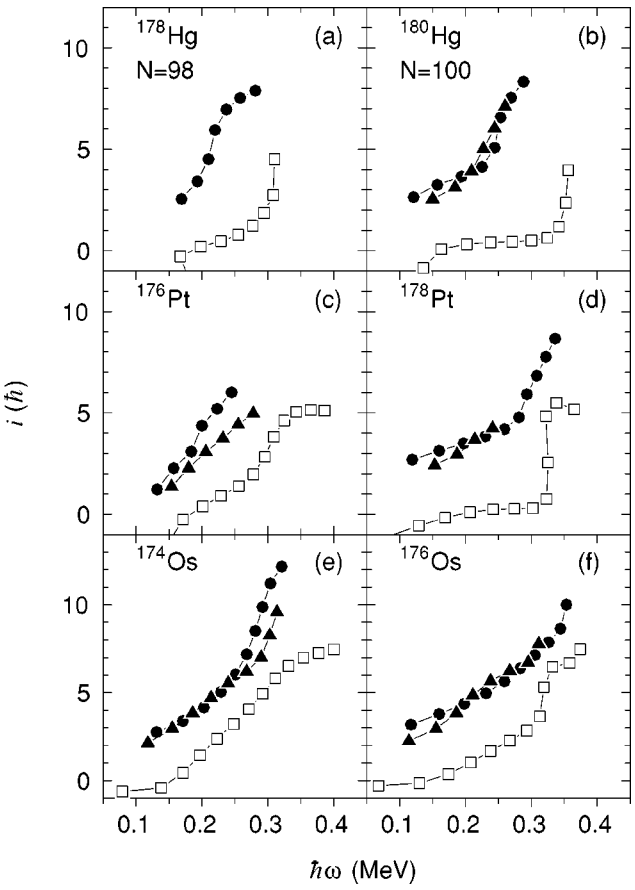

FIG. 6. Aligned angular momenta for the ground-state bands (open symbols) and the negative parity bands (filled symbols) in the $N=98$ and 100 Os, Pt, and Hg isotones. Reference parameters of $\mathfrak{I}_0 = 29$ MeV$^{-1}\hbar^2$ and $\mathfrak{I}_1 = 200$ MeV$^{-3}\hbar^4$ have been used for the bands in ^{178}Hg, of $\mathrm{Im}_0 = 29$ MeV$^{-1}\hbar^2$ and $\mathfrak{I}_1 = 160$ MeV$^{-3}\hbar^4$ for the bands in ^{180}Hg, ^{176}Pt, and ^{178}Pt, and of $\mathfrak{I}_0 = 26$ MeV$^{-1}\hbar^2$ and $\mathfrak{I}_1 = 120$ MeV$^{-3}\hbar^4$ for the bands in ^{174}Os and ^{176}Os.

A careful inspection of the level schemes of the heavier even-even Hg isotopes with neutron number $N = 98-106$ reveals that in each nucleus a band of negative parity can be found with characteristics resembling closely those enumerated above. Furthermore, this observation can also be extended to the even-even Os and Pt isotones. Figure 5 presents the excitation energies of the 5^- through 13^- members of the sidebands of interest in the three isotopic chains. Clearly, the variations with N of the excitation energies are small and very similar in all the nuclei under consideration. This observation argues against a pure two-quasiparticle character for these structures, and supports their association with octupole vibrations. The enhancement of the octupole correlations at low spin in this mass region comes as no surprise because of the presence of pairs of orbitals with $\Delta j = \Delta l = 3\hbar$ near both the proton and the neutron Fermi surfaces (see, for example, Ref. [33] and references therein). In fact, the specific configurations contributing to the structure of the octupole phonon have recently been discussed in some detail by Kondev *et al.* [18]. It is worth pointing out that the negative parity bands decay mostly but not exclusively via $E1$ transitions where the $J \rightarrow J+1$ branches are strongly favored.

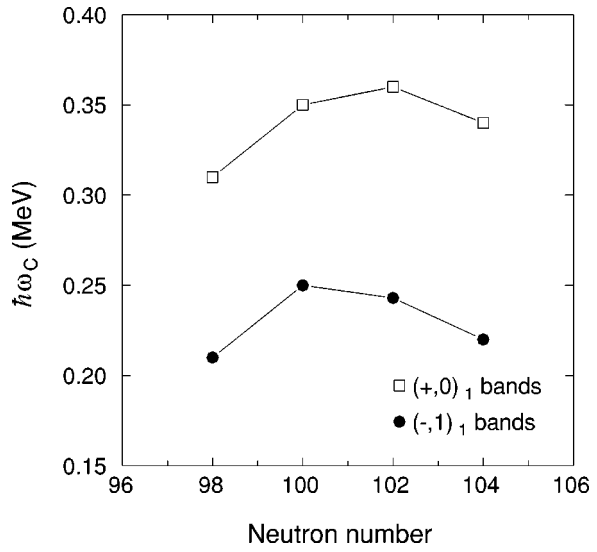

FIG. 7. Crossing frequencies for the ground-state bands (open squares) and the negative parity bands (filled circles) in even-even Hg nuclei. The errors on the extracted frequencies are of the order of 10%.

As detailed in Refs. [13,20], this property is consistent with expectation for octupole vibrational structures.

The alignment i, as a function of the rotational frequency $\hbar\omega$, for band structures in the Os, Pt, and Hg isotones with $N=98$ and 100 is presented in Fig. 6. From this figure, it is clear that the alignments of bands 2 and 3 in ^{180}Hg follow the same pattern with frequency. Hence, the bands can be associated with the same configuration and be interpreted as signature partners with significant splitting [suggesting that the configuration has a low K quantum number ($K=0$ or 1)]. In all nuclei, the ground-state band exhibits a crossing around $\hbar\omega\sim 0.32$ MeV. The dependence of the crossing frequency with mass for the Hg isotopes is given in Fig. 7. This crossing can be attributed to the alignment of a pair of $i_{13/2}$ neutrons and the small variations with mass are due to small differences in the respective deformations [34]. The striking similarity between the properties of the negative-parity bands at low spin is also clearly visible in this figure: in all cases the band built on the octupole excitation (responsible for the $3\hbar$ alignment at low frequency) follows a trajectory in the i vs $\hbar\omega$ plane similar to that of the yrast line before a crossing occurs. In the Hg isotopes (Fig. 7) the crossing frequency for the negative parity band is distinctly lower than that of the yrast sequence. This systematic observation does not hold for the Pt and Os isotopic chains (not shown) and suggests that the nature of the crossing band may well be different. Vogel [35] suggested initially that the crossing excitation is associated with a two-quasiparticle excitation. The issue, then, is to identify the exact structure of the two-quasiparticle band in the Hg isotopes.

In order to predict which intrinsic configurations are involved in the Hg isotopes, calculations of the energies of the lowest two-quasiparticle states were carried out using the approach outlined in Ref. [36] and applied recently to the case of ^{178}Pt in Ref. [18] (where relevant details about the method can be found). Representative results of the calculations are presented in Table V for the case of ^{178}Hg. The conclusions that can be drawn from these predictions are similar for ^{180}Hg. From Table V it is clear that the lowest neutron excitations of negative parity involve the $i_{13/2}$ orbital. Any two-quasineutron configuration involving a single $i_{13/2}$ neutron will not result in an alignment of the magnitude seen in the data of Fig. 6. Thus, it appears unlikely that the high-frequency part of the negative parity bands can be readily associated with a neutron excitation. The calculations (Table V) also show that two-quasiproton configurations are present in the vicinity of the Fermi surface and protons become the preferred candidates for the excitation crossing the octupole bands.

TABLE V. Calculated excitation energies for low-lying negative-parity, two-quasiparticle configurations in ^{178}Hg. The present results were obtained for deformation parameters of $\beta_2=0.247$ and $\beta_4=-0.015$.

Configuration [a]		K^{π}_{-} [b]	E^{qp}_{-}	K^{π}_{+} [b]	E^{qp}_{+}
π^2	ν^2		(keV) [c]		(keV) [c]
(**1/2**$^-$, **1/2**$^+$)		0^-	2710	1^-	2310
(**1/2**$^{-\prime}$, **1/2**$^+$)		0^-	2416	$\underline{1^-}$	2816
(**1/2**$^-$, 3/2$^+$)		$\underline{1^-}$	2191	2^-	2591
(**1/2**$^{-\prime}$, 3/2$^+$)		$\underline{1^-}$	2690	2^-	2290
(**3/2**$^-$, 3/2$^+$)		0^-	2355	$\underline{3^-}$	2755
(**1/2**$^-$, 1/2$^+$)		$\underline{0^-}$	2679	1^-	2279
(**1/2**$^{-\prime}$, 1/2$^+$)		0^-	2384	$\underline{1^-}$	2784
(5/2$^+$, 9/2$^-$)		$\underline{2^-}$	3276	7^-	3676
	(5/2$^-$, **5/2**$^+$)	$\underline{0^-}$	1666	5^-	2018
	(5/2$^-$, **7/2**$^+$)	$\underline{1^-}$	1833	6^-	2269
	(5/2$^-$, **9/2**$^+$)	$\underline{2^-}$	3270	7^-	3638

[a]Protons (π): **1/2**$^-$: 1/2$^-$[541] ($h_{9/2}$), **3/2**$^-$: 3/2$^-$[532]($h_{9/2}$), **1/2**$^{-\prime}$: 1/2$^-$[530] ($f_{7/2}$), 9/2$^-$: 9/2$^-$[514] ($h_{11/2}$),1/2$^+$: 1/2$^+$[400]($s_{1/2}$), 3/2$^+$: 3/2$^+$[402] ($d_{3/2}$), **1/2**$^+$: 1/2$^+$[660] ($i_{13/2}$); neutrons (ν): 1/2$^-$: 1/2$^-$[521] ($p_{3/2}$), 5/2$^-$: 5/2$^-$[512] ($f_{7/2}$), 7/2$^-$: 7/2$^-$[514] ($h_{9/2}$), **5/2**$^+$: 5/2$^+$[642] ($i_{13/2}$), **7/2**$^+$: 7/2$^+$[633] ($i_{13/2}$); **9/2**$^+$: 9/2$^+$[624] ($i_{13/2}$).

[b]$K_{\pm}=|\Omega_{\pi_1(\nu_1)}\pm\Omega_{\pi_2(\nu_2)}|$. The expected energetically favored states are underlined.

[c]Due to the rapid downslope of the $h_{9/2}$, $f_{7/2}$, and $i_{13/2}$ proton orbitals as deformation increases, the excitation energy of configurations which involve these structures are strongly deformation dependent.

Because of the softness of the potential in the Hg isotopes, as evidenced by their susceptibility to shape changes, total Routhian surface (TRS) calculations based on a Woods-Saxon potential were performed following the procedure outlined in Ref. [37] in order to trace in deformation space the evolution with rotational frequency of the various configurations. Sample results are given in Table VI for all the $N=98-106$ even-even Hg nuclei at a frequency of ~ 0.2 MeV relevant for the present discussion. Calculated deformations are presented for the ground-state (i.e. vacuum) band, as well as for the two-quasineutron $i^2_{13/2}$ configuration (AB) which crosses it. In addition, similar information is provided for the

TABLE VI. Calculated equilibrium deformations, β_2, γ, β_4 from the TRS calculations for selected configurations in even-even Hg isotopes at $\hbar\omega \sim 0.20$ MeV (see the text for details).

Nucleus	Configuration											
	Vacuum			af			AF			AB		
	β_2	γ (deg)	β_4	β_2	γ (deg)	β_4	β_2	γ (deg)	β_4	β_2	γ (deg)	β_4
^{178}Hg	0.242	−4.6	0.0274	0.256	11.0	0.0289	0.241	−3.6	0.0244	0.222	−12.7	0.0180
^{180}Hg	0.265	−4.6	0.0183	0.260	9.3	0.0192	0.265	−2.7	0.0160	0.242	−11.8	0.0098
^{182}Hg	0.272	−1.9	0.0061	0.269	5.3	0.0081	0.262	−2.6	0.0030	0.241	−11.1	−0.0025
^{184}Hg	0.262	−4.1	−0.0072	0.260	8.2	−0.0057	0.252	−5.1	−0.0106	0.239	−13.0	−0.0128
^{186}Hg	0.241	−7.4	−0.0206	0.249	12.5	−0.0188	0.246	−3.7	−0.0229	0.229	−11.2	−0.0256

lowest two-quasiproton $[\pi^2(i_{13/2}\otimes h_{9/2}),\ af]$ and two-quasineutron $[\nu^2(i_{13/2}\otimes f_{7/2}),\ AF]$ configurations. The TRS calculations indicate that this two-quasiproton excitation, labeled by the Nilsson asymptotic quantum numbers $\pi^2([660]1/2^+\otimes[541]1/2^-)$, drives ^{178}Hg from the yrast deformation of $\beta_2=0.24$, $\gamma=-5°$ towards a slightly more deformed shape with a larger degree of triaxiality; $\beta_2=0.26$, $\gamma=11°$. A similar trend can be seen for ^{180}Hg. With the orbitals involved, the large alignment measured experimentally ($\sim 8\hbar$) at high frequency is accounted for. However, as already pointed out in Ref. [24], it should be realized that this $\pi^2(i_{13/2}\otimes h_{9/2})$ excitation is not the only possible one. In particular, from studies of the light, odd-even Au isotopes [38,39], the $[530]1/2^-$ state (of predominant $f_{7/2}$ parentage) has also been identified. Hence, a $\pi^2(i_{13/2}\otimes f_{7/2})$ two-quasiproton configuration cannot be ruled out. Furthermore, sizable mixing between these $\pi^2(i_{13/2}\otimes h_{9/2})$ and $\pi^2(i_{13/2}\otimes f_{7/2})$ configurations is also possible.

The microscopic structure of the octupole phonon is probably rather complex with contributions of various orbitals fulfilling the $\Delta j=\Delta l=3$ condition. It is likely, however, that the proton $i_{13/2}\otimes f_{7/2}$ coupling will be an important component (see Ref. [18]). If so, the shape driving effects of the $i_{13/2}$ orbital described above will remain strong and the nuclear shape associated with the low-spin part of the negative parity bands may well be similar to the one associated with the two-quasiproton configuration. Thus, the deformation would be somewhat different from that of the vacuum configuration. This, in turn, would provide a qualitative explanation for the fragmented decay observed at low spin in band 2.

V. SUMMARY AND CONCLUSIONS

Extended level schemes for ^{178}Hg and ^{180}Hg were obtained by combining the selectivity of the FMA with the high detection efficiency and resolving power of the Gammasphere spectrometer. The ground-state bands were observed to moderate spin ($I\geqslant 20\ \hbar$) and they exhibit the usual first crossing which is attributed to the alignment of a pair of $i_{13/2}$ neutrons. The excited sidebands were assigned odd spin and negative parity. The configurations of these structures were interpreted as octupole vibrations at low spin which are crossed at higher frequency by two-quasiproton excitations.

ACKNOWLEDGMENTS

The authors wish to thank the staff of the ATLAS accelerator facility and the Physics Support Group for their assistance in various phases of the experiment. We are grateful to J. P. Greene for help with the targets. The software support by D. C. Radford and H. Q. Jin is greatly appreciated. Discussions with W. Nazarewicz, P.-H. Heenen, M. A. Riley, and G. D. Dracoulis are gratefully acknowledged. S.S. acknowledges support from a NATO grant through the Research Council of Norway. This work was supported by the U.S. Department of Energy, Nuclear Physics Division, under Contracts No. W-31-109-ENG-38, DE-FG02-96ER40983, DE-FG02-95ER40939, and DE-FG05-88ER40406.

[1] J. L. Wood, K. Heyde, W. Nazarewicz, M. Huyse, and P. Van Duppen, Phys. Rep. **215**, 103 (1992), and references therein; J. H. Hamilton, P. G. Hansen, and E. F. Zganjar, Rep. Prog. Phys. **48**, 631 (1985).
[2] K. Heyde, P. Van Isacker, M. Waroquier, J. L. Wood, and R. A. Meyer, Phys. Rep. **102**, 293 (1983).
[3] I. G. Bearden *et al.*, Nucl. Phys. **A576**, 441 (1994).
[4] X. L. Han and C. L. Wu, At. Data Nucl. Data Tables **73**, 43 (1999).
[5] E. S. Paul *et al.*, Phys. Rev. C **51**, 78 (1995); R. S. Simon *et al.*, Z. Phys. A **325**, 197 (1986).
[6] M. P. Carpenter *et al.*, Phys. Rev. Lett. **78**, 3650 (1997).
[7] M. Muikku *et al.*, Phys. Rev. C **58**, R3033 (1998).
[8] G. D. Dracoulis *et al.*, Phys. Lett. B **208**, 365 (1988).
[9] R. Bengtsson, T. Bengtsson, J. Dudek, G. Leander, W. Nazarewicz, J.-Y. Zhang, Phys. Lett. B **183**, 1 (1987).
[10] W. Nazarewicz, Phys. Lett. B **305**, 195 (1993).
[11] W. C. Ma *et al.*, Phys. Rev. C **47**, R5 (1993).
[12] R. V. F. Janssens and T. L. Khoo, Annu. Rev. Nucl. Part. Sci. **41**, 321 (1991).
[13] G. D. Dracoulis, J. Phys. (Paris) C **10**, c10 (1980).
[14] G. D. Dracoulis, C. Fahlander, and M. P. Fewell, Nucl. Phys. **A383**, 119 (1982).
[15] R. M. Lieder *et al.*, Nucl. Phys. **A645**, 465 (1999).
[16] C. Fahlander and G. D. Dracoulis, Nucl. Phys. **A375**, 263 (1982).

[17] B. Cederwall *et al.*, Z. Phys. A **337**, 283 (1990).
[18] F. G. Kondev *et al.*, Phys. Rev. C **61**, 044323 (2000).
[19] F. Soramel *et al.*, Eur. Phys. J. A **4**, 17 (1999).
[20] M. J. A. de Voigt, R. Kaczarowski, H. J. Riezebos, R. F. Noorman, J. C. Bacelar, M. A. Deleplanque, R. M. Diamond, F. S. Stephens, J. Sauvage, and B. Roussiére, Nucl. Phys. **A507**, 472 (1990).
[21] D. G. Popescu *et al.*, Phys. Rev. C **55**, 1175 (1997).
[22] K. S. Bindra *et al.*, Phys. Rev. C **51**, 401 (1995).
[23] J. K. Deng *et al.*, Phys. Rev. C **52**, 595 (1995).
[24] F. G. Kondev *et al.*, Phys. Rev. C **61**, 011303(R) (2000).
[25] F. G. Kondev *et al.* (unpublished).
[26] I. Y. Lee, Nucl. Phys. **A520**, 641c (1990).
[27] C. N. Davids, B. B. Back, K. Bindra, D. J. Henderson, W. Kutschera, T. Lauritsen, Y. Nagame, P. Sugathan, A. V. Ramayya, and W. B. Walters, Nucl. Instrum. Methods Phys. Res. B **70**, 358 (1992).
[28] D. C. Radford, Nucl. Instrum. Methods Phys. Res. A **361**, 297 (1995).
[29] Y. A. Akovali, Nucl. Data Sheets **84**, 1 (1998).
[30] W. R. Leo, *Techniques for Nuclear and Particle Physics Experiments: A How-to Approach* (Springer-Verlag, Berlin, 1987), p. 105.
[31] R. A. Bark, G. D. Dracoulis, and A. E. Stuchbery, Nucl. Phys. **A514**, 503 (1990).
[32] B. Fabricius, G. D. Dracoulis, R. A. Bark, A. E. Stuchbery, T. Kibédi, and A. M. Baxter, Nucl. Phys. **A511**, 345 (1990).
[33] P. A. Butler and W. Nazarewicz, Rev. Mod. Phys. **68**, 349 (1996).
[34] R. Wyss, W. Satula, W. Nazarewicz, and A. Johnson, Nucl. Phys. **A511**, 324 (1990).
[35] P. Vogel, Phys. Lett. **60B**, 431 (1976).
[36] F. G. Kondev, G. D. Dracoulis, A. P. Byrne, T. Kibédi, and S. Bayer, Nucl. Phys. **A617**, 91 (1997).
[37] M. P. Carpenter *et al.*, Nucl. Phys. **A513**, 125 (1990).
[38] F. G. Kondev *et al.* (unpublished).
[39] W. F. Mueller *et al.*, Phys. Rev. C **59**, 2009 (1999).